AD-A191 643 EVALUATION OF THE BIOT COEFFICIENTS(U) TEXAS UNIV AT AUSTIN APPLIED RESEARCH LABS B YAVARI ET AL 1987 1/1
N00014-86-K-0387

UNCLASSIFIED F/G 20/1 NL

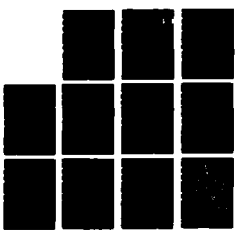

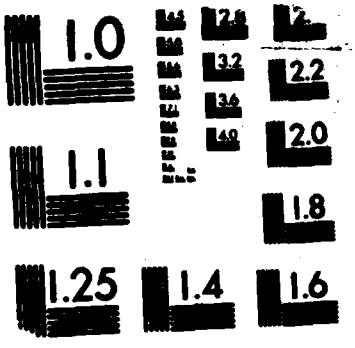

Final Technical Report on ONR Contract N00014-86-K-0387

EVALUATION OF THE BIOT COEFFICIENTS

B. Yavari and A. Bedford
Applied Research Laboratories and
Aerospace Engineering and Engineering Mechanics Department
The University of Texas at Austin
Austin, Texas 78712

Abstract

The Biot equations are the most promising approach for modeling the propagation of acoustic waves in ocean sediments. A method has been developed by Bedford, Costley and Stern for determining the drag and virtual mass coefficients in Biot's equations as functions of frequency. The method requires solving for the motion of the fluid in the pores when the pore walls are subjected to a spatially uniform, oscillatory motion. In this project, a finite element algorithm has been developed to determine the fluid motion. The accuracy of the model has been verified using a model problem for which exact results could be obtained. The drag and virtual mass coefficients have been determined for several two dimensional pore spaces. It has been determined that the drag coefficient is insensitive to the pore geometry while the virtual mass coefficient is very sensitive to the pore geometry. It has also been shown that the coefficients can be expressed in nondimensional forms which permit their values to be scaled for different values of a characteristic linear dimension of the pore space. This project has established a firm basis for proceeding to determine the coefficients for three dimensional pore spaces.

Introduction

Biot (1956a, 1956b) developed a theory to model the propagation of acoustic waves in fluid saturated porous media. It has been shown by numerous investigators that the Biot theory correctly predicts many of the acoustical properties of fluid saturated porous media; see, for example, Berryman (1969), Hovem & Ingram (1979), Johnson & Plona (1982), Stoll (1977), and Stoll & Bryan (1969). As a result, this theory is regarded by many investigators to be the most promising avenue for the study of waves in saturated porous media.

However, an important question remains to be answered. It is known that the coefficients in Biot's equations depend upon the wave frequency, and they also depend on the fabric, or microstructure, of the solid constituent. Until these coefficients can be determined as functions of frequency, an important obstacle to the accurate comparison of the Biot theory with acoustic measurements in porous media will remain.

Recently, Bedford, Costley, & Stern (1984) proposed a technique for evaluating the drag and virtual mass coefficients in Biot's equations as functions of frequency. The method requires solving for the motion of the fluid in the pores when the pore walls are subjected to a spatially uniform, oscillatory motion. To evaluate the method, Bedford (1986) has applied it to a medium consisting of alternating plane layers of fluid and solid. For this simple medium, the drag and virtual mass coefficients could be determined in closed form. Furthermore, in this case the phase velocity and attenuation of plane waves could be determined exactly.

It was found that when the drag and virtual mass coefficients were determined using the method of Bedford, Costley & Stern, the velocity and attenuation of the fast and slow waves predicted by the Biot theory agreed extremely closely with the first two modes of the exact solution over a large range of frequencies. However, when the virtual mass coefficient was assumed to be independent of frequency (which is currently done by most investigators), the Biot theory accurately predicted the velocity and attenuation only at very low frequency.

With these results as motivation, a program of research has been initiated to use the finite element method together with the method of Bedford, Costley & Stern to determine the Biot drag and virtual mass coefficients

for realistic pore spaces. In this paper, the finite element formulation is described and used to determine the coefficients as functions of frequency for various two dimensional pore spaces.

The Method

The one dimensional forms of Biot's equations can be written (Biot 1956a)

$$\begin{aligned}(1-\phi)\rho_s\ddot{u}_s &= (P+2\mu)\frac{\partial^2 u_s}{\partial x^2} + Q\frac{\partial^2 u_f}{\partial x^2} \\ &\quad -b(\dot{u}_s-\dot{u}_f) - c(\ddot{u}_s-\ddot{u}_f) + f_s, \\ \phi\rho_f\ddot{u}_f &= Q\frac{\partial^2 u_s}{\partial x^2} + R\frac{\partial^2 u_f}{\partial x^2} \\ &\quad +b(\dot{u}_s-\dot{u}_f) + c(\ddot{u}_s-\ddot{u}_f) + f_f.\end{aligned} \tag{1}$$

The first equation is the equation of motion of the solid constituent. The term ϕ is the porosity (the pore volume per unit volume of the porous medium). The terms ρ_s and u_s are the density and the displacement of the solid material. The terms P, μ, Q and R are constitutive coefficients which depend on the properties of the fluid and solid constituents. The terms containing b and c are forces exerted on the solid constituent by the fluid constituent due to their relative motion. The term containing b is linear in the relative velocity, and b is the drag coefficient. The term containing c is linear in the relative acceleration. This is called a "virtual mass" force, and c is the virtual mass coefficient. The second equation is the equation of motion of the fluid constituent. The terms ρ_f and u_f are the density and the displacement of the fluid. The terms f_s and f_f are external body force densities.

Consider an imaginary experiment in which the solid constituent is given a *spatially uniform*, steady state oscillatory motion

$$u_s = D\,e^{i\omega t}, \tag{2}$$

where D is a real constant and ω is the frequency. This could be achieved (hypothetically) by applying a suitably prescribed external body force density f_s. The resulting steady state motion of the fluid will be of the form

$$u_f = U e^{i\omega t}, \tag{3}$$

where U is a complex constant. Substituting these two expressions for u_s and u_f into the Biot equation of motion for the fluid constituent $(1)_2$ gives the result

$$\phi\rho_f\omega U = (ib - \omega c)(U - D). \tag{4}$$

The terms in the equation $(1)_2$ containing Q and R vanish because the motion is spatially uniform. The complex equation (4) can be solved for the two real coefficients b and c, yielding

$$\begin{aligned} b &= \phi\rho_f\omega \,\text{Imaginary}[\tilde{U}/(\tilde{U}-1)], \\ c &= -\phi\rho_f \,\text{Real}[\tilde{U}/(\tilde{U}-1)], \end{aligned} \tag{5}$$

where $\tilde{U} = U/D$. If the term $\tilde{U}$ is known as a function of frequency, Eqs. (5) can be solved for b and c as functions of frequency. Thus determining b and c reduces to the solution of a steady state boundary value problem in fluid mechanics: give the boundary of the pore volume of a porous medium a spatially uniform, oscillatory motion (2) and determine the motion of the fluid within. The volumetric average of the fluid displacement is identified with the fluid displacement u_f in Biot's equations. In this way, $\tilde{U}$ can be determined as a function of frequency.

Biot (1956b) determined the drag coefficient as a function of frequency by subjecting the pore fluid in a straight, cylindrical pore to a oscillatory pressure gradient. His method was extended by Hovem & Ingram (1979) to determine the virtual mass coefficient as a function of frequency. Bedford, Costley & Stern (1984) made numerical comparisons of the results of their method for the case of a cylindrical pore and found that they were identical to those of Biot and of Hovem & Ingram.

Can the coefficients determined as functions of frequency in this way be applied to the problem of waves propagating in the medium? To investigate this question, the method has been applied to a medium consisting of alternating plane layers of fluid and solid (Bedford 1986). The material properties and the layer thicknesses were chosen to correspond to water saturated sand. In Figs. 1 and 2, the phase velocity and attenuation of the fast wave predicted by Biot's equations are compared to the first mode of the exact solution for compressional waves propagating parallel to the layers. When the drag and virtual mass coefficients are determined using the method of Bedford, Costley and Stern, the Biot theory matches the

exact solution very closely up to a frequency of 1 MHz. (The curves are indistinguishable.) However, when the virtual mass coefficient is assumed to be constant, the Biot theory agrees with the exact solution only at very low frequency.

Since the coefficients are determined by subjecting the solid constituent to a spatially uniform oscillation, the results will clearly be applicable to propagating waves only when wavelengths are large in comparison to a characteristic linear dimension of the pore space. However, this is not an important restriction since the Biot theory itself is subject to the same condition.

Finite Element Formulation

The Boundary Value Problem

The method of Bedford, Costley & Stern requires that the motion of the viscous, compressible fluid in the pore space of a porous medium be determined when the pore walls are given a spatially uniform, oscillatory motion. In this paper the motion of the fluid is determined by using the finite element method. (See, for example, Becker *et al.* 1981.)

Under the assumption of small displacements, a viscous compressible fluid is governed by the equation

$$\rho_f \ddot{\mathbf{u}} = -\nabla p + (\kappa + \tfrac{1}{3}\eta)\nabla(\nabla \cdot \dot{\mathbf{u}}) + \eta \nabla^2 \dot{\mathbf{u}}. \tag{6}$$

The vector $\mathbf{u}$ is the displacement of the fluid, p is the pressure, κ is the bulk viscosity, and η is the viscosity. The pressure is related to the dilatation of the fluid by

$$p = -K \nabla \cdot \mathbf{u}, \tag{7}$$

where K is the bulk modulus of the fluid.

The boundary condition imposed at the boundary of the pore space is

$$\mathbf{u} = D\, e^{i\omega t} \mathbf{e}_1, \tag{8}$$

where $\mathbf{e}_1$ is a unit vector that specifies the direction of the oscillatory motion of the boundary and ω is the frequency. The resulting steady state solutions

for the displacement and pressure can be written

$$\begin{aligned} \mathbf{u} &= \bar{\mathbf{u}} e^{i\omega t}, \\ p &= \bar{p} e^{i\omega t}. \end{aligned} \tag{9}$$

Substituting these solutions into Eqs. (6) and (7), the steady state boundary value problem reduces to

$$\left.\begin{aligned} A\nabla^2\bar{\mathbf{u}} + B\nabla(\nabla\cdot\bar{\mathbf{u}}) + \bar{\mathbf{u}} &= 0 \\ \nabla\cdot\bar{\mathbf{u}} &= -\bar{p}/K \end{aligned}\right\} \quad \text{in } \Omega$$
$$\bar{\mathbf{u}} = D\,\mathbf{e}_1 \qquad \text{on } \partial\Omega \tag{10}$$

where Ω is the domain (the volume) in which the solution is to be obtained, $\partial\Omega$ is the surface of Ω, and A and B are defined by

$$\begin{aligned} A &= i\eta/(\rho_f\omega), \\ B &= K/(\rho_f\omega^2) + i(\kappa + \tfrac{1}{3}\eta)/(\rho_f\omega). \end{aligned} \tag{11}$$

The Variational Formulation

Multiplying Eq. $(10)_1$ by a variation $\delta\bar{\mathbf{u}}$ and integrating over the domain yields the variational expression

$$\int_\Omega [A\nabla^2\bar{\mathbf{u}} + B\nabla(\nabla\cdot\bar{\mathbf{u}}) + \bar{\mathbf{u}}]\cdot\delta\bar{\mathbf{u}}\,dv = 0. \tag{12}$$

By integrating by parts, this equation can be written

$$\int_\Omega [A\nabla\bar{\mathbf{u}} : \nabla\delta\bar{\mathbf{u}} + B(\nabla\cdot\bar{\mathbf{u}})(\nabla\cdot\delta\bar{\mathbf{u}}) - \bar{\mathbf{u}}\cdot\delta\bar{\mathbf{u}}]\,dv = 0, \tag{13}$$

where the notation $\nabla\bar{\mathbf{u}} : \nabla\delta\bar{\mathbf{u}}$ denotes the product

$$\nabla\bar{\mathbf{u}} : \nabla\delta\bar{\mathbf{u}} = \sum_i \sum_j \frac{\partial\bar{u}_i}{\partial x_j}\frac{\partial\delta\bar{u}_i}{\partial x_j}.$$

Let a functional $\pi(\bar{\mathbf{u}})$ be defined by

$$\pi(\bar{\mathbf{u}}) = \tfrac{1}{2}\int_\Omega [A\nabla\bar{\mathbf{u}} : \nabla\bar{\mathbf{u}} + B(\nabla\cdot\bar{\mathbf{u}})(\nabla\cdot\bar{\mathbf{u}}) - \bar{\mathbf{u}}\cdot\bar{\mathbf{u}}]\,dv. \tag{14}$$

At small frequencies, the change in density of the fluid and consequently the dilatation $\nabla\cdot\bar{\mathbf{u}}$ are very small. This results in computational difficulties

which can be avoided by expressing the problem in a form suitable for a nearly incompressible material (Herrman 1965). Equation $(10)_2$ is introduced into the functional (14) as a constraint by introducing a Lagrange multiplier λ. This results in an "augmented" functional defined by

$$\pi^*(\bar{\mathbf{u}}, \lambda, \bar{p}) = \tfrac{1}{2}\int_\Omega [A\nabla\bar{\mathbf{u}} : \nabla\bar{\mathbf{u}} - (B/K)\bar{p}\nabla\cdot\bar{\mathbf{u}} - \bar{\mathbf{u}}\cdot\bar{\mathbf{u}} + 2\lambda(\nabla\cdot\bar{\mathbf{u}} + \bar{p}/K)]\, dv. \tag{15}$$

By equating the variation of this expression to zero, it can be shown that $\lambda = -B\bar{p}/(2K)$. Substituting this result into the augmented functional, it can be written

$$\pi^*(\bar{\mathbf{u}}, \bar{p}) = \tfrac{1}{2}\int_\Omega [A\nabla\bar{\mathbf{u}} : \nabla\bar{\mathbf{u}} - (2B\bar{p}/K)\nabla\cdot\bar{\mathbf{u}} - (B/K^2)\bar{p}^2 - \bar{\mathbf{u}}\cdot\bar{\mathbf{u}}]\, dv. \tag{16}$$

Taking the variation of this expression yields the variational formulation

$$\delta\pi^* = \int_\Omega [A\nabla\bar{\mathbf{u}} : \nabla\delta\bar{\mathbf{u}} - (B/K)(\nabla\cdot\bar{\mathbf{u}}\,\delta\bar{p} + \bar{p}\nabla\cdot\delta\bar{\mathbf{u}}) - (B/K^2)\bar{p}\,\delta\bar{p} - \bar{\mathbf{u}}\cdot\delta\bar{\mathbf{u}}]\, dv = 0. \tag{17}$$

The Finite Element Approximation

A finite element approximation is obtained by replacing the domain Ω in Eq. (17) by a discretized domain Ω_h. The objective is to seek approximate solutions $\bar{\mathbf{u}}_h$ and $\bar{p}_h$ which depend upon the mesh size of the discretized domain. The solution $\bar{\mathbf{u}}_h$ is assumed to be contained in a subspace of $H^1(\Omega_h)$, and the solution $\bar{p}_h$ is assumed to be contained in a subspace of $H^0(\Omega_h)$, where $H^n(\Omega_h)$ denotes the set of functions on Ω_h whose nth derivatives are square integrable. Equation (17) becomes

$$\int_{\Omega_h} [A\nabla\bar{\mathbf{u}}_h : \nabla\delta\bar{\mathbf{u}}_h - (B/K)(\nabla\cdot\bar{\mathbf{u}}_h\,\delta\bar{p}_h + \bar{p}_h\nabla\cdot\delta\bar{\mathbf{u}}_h) - (B/K^2)\bar{p}_h\,\delta\bar{p}_h - \bar{\mathbf{u}}_h\cdot\delta\bar{\mathbf{u}}_h]\, dv = 0. \tag{18}$$

In terms of suitable finite element basis functions Ψ_i and Θ_i,the approximate solutions can be written

$$\bar{\mathbf{u}}_h = \sum_i \Psi_i\bar{\mathbf{U}}_i, \quad \bar{p}_h = \sum_i \Theta_i\bar{P}_i, \tag{19}$$

where $\bar{\mathbf{U}}_i$ and $\bar{P}_i$ are the nodal point values of $\bar{\mathbf{u}}_h$ and $\bar{p}_h$ respectively. Substituting the expressions (19) into Eq. (18) yields the linear system of equations

$$\begin{bmatrix} K_{11} & K_{12} \\ K_{12} & K_{22} \end{bmatrix} \begin{bmatrix} \bar{\mathbf{U}} \\ \bar{P} \end{bmatrix} = 0, \tag{20}$$

where

$$\begin{aligned} (K_{11})_{ij} &= \int_{\Omega_h} [A\nabla\Psi_i : \nabla\Psi_j - \Psi_i\Psi_j]\, dv, \\ (K_{12})_{ij} &= \int_{\Omega_h} [-(B/K)\nabla\cdot\Psi_i\Theta_j]\, dv, \\ (K_{22})_{ij} &= \int_{\Omega_h} [-(B/K^2)\Theta_i\Theta_j]\, dv \end{aligned} \tag{21}$$

Equations (20) have been solved by applying the essential boundary conditions $\bar{\mathbf{u}} = D\,\mathbf{e}_1$ on the pore boundaries and periodic boundary conditions where the domains of interest exhibit periodicity.

Scaling

Determining the Biot drag and virtual mass coefficients as functions of frequency by the method described here requires a substantial investment in computer time. An important question is whether, once the coefficients have been determined for a particular fabric or microstructure, the results can be scaled if the characteristic linear dimension of the pore space changes. For example, if the coefficients were determined for the case of spherical grains with a particular packing, can the results be scaled to determine the coefficients for spherical grains of the same packing but a different diameter? In this section it is shown that the answer to this question is yes, at least within a particular range of frequencies and microdimensions.

By substituting Eq. (7) into Eq. (6), the equation of motion of the viscous compressible fluid in the pores can be written in terms of the displacement components u_k as

$$\rho_f \frac{\partial^2 u_k}{\partial t^2} = K\frac{\partial^2 u_i}{\partial x_i \partial x_k} + (\kappa + \tfrac{1}{3}\eta)\frac{\partial^2 u_i}{\partial x_i \partial x_k} + \eta\frac{\partial^2 u_k}{\partial x_i \partial x_i}. \tag{22}$$

In terms of the steady state solution $u_k = \bar{u}_k e^{i\omega t}$, this is

$$-\omega^2 \rho_f \bar{u}_k = K \frac{\partial^2 \bar{u}_i}{\partial x_i \partial x_k} + i\omega(\kappa + \tfrac{1}{3}\eta) \frac{\partial^2 \bar{u}_i}{\partial x_i \partial x_k} + i\omega\eta \frac{\partial^2 \bar{u}_k}{\partial x_i \partial x_i}. \tag{23}$$

Let D be a characteristic linear dimension of the pore space, and let dimensionless displacements and coordinates be defined by

$$\tilde{u}_k \equiv \bar{u}_k / D, \quad \tilde{x}_k \equiv x_k / D. \tag{24}$$

In terms of these dimensionless quantities, Eq. (23) can be written

$$-\tilde{u}_k = \left\{ \left[\frac{1}{M^2} \right] + i \left[\frac{1}{Re'} \right] \right\} \frac{\partial^2 \tilde{u}_i}{\partial \tilde{x}_i \partial \tilde{x}_k} + i \left[\frac{1}{Re} \right] \frac{\partial^2 \tilde{u}_k}{\partial \tilde{x}_i \partial \tilde{x}_i}, \tag{25}$$

where

$$M = \frac{\omega D}{(K/\rho_f)^{\frac{1}{2}}}, \quad Re = \frac{\rho_f \omega D^2}{\eta}, \quad Re' = \frac{\rho_f \omega D^2}{\kappa + \frac{1}{3}\eta}. \tag{26}$$

It is seen that the equation which governs the dimensionless displacement $\tilde{u}_k$ (and therefore the dimensionless average displacement in the direction of motion $\tilde{U}$) is characterized by three dimensionless groups. The dimensionless group M can be recognized as a Mach number (the term $(K/\rho_f)^{\frac{1}{2}} \equiv c$ is the speed of sound in the fluid), and the dimensionless groups Re and Re' are Reynolds numbers. This result together with Eqs. (5) for b and c leads to the conclusion that the quantities $b/(\phi\rho_f\omega)$ and $c/(\phi\rho_f)$ can be expressed as functions of M, Re and Re'.

The Mach number M is a measure of the effect on the solution of the compressibility of the fluid. For frequencies that are sufficiently low that $M^2 \ll 1$, the effect of compressibility can be neglected and the quantities $b/(\phi\rho_f\omega)$ and $c/(\phi\rho_f)$ can be expressed as functions of Re alone. (The analogy with gas dynamics is obvious.)

For this reason, the principle results will be presented in the next section as plots of the dimensionless drag coefficient $b/(\phi\rho_f\omega)$ and dimensionless virtual mass coefficient $c/(\phi\rho_f)$ as functions of the "dimensionless frequency" Re. This makes the results independent of the properties of the fluid, and also makes them independent of the characteristic linear dimension D so long as the restriction $M^2 \ll 1$ is satisfied. It must be emphasized that this restriction refers to the frequency range within which the results can be scaled. The computations that have been made did account for the compressibility of the fluid.

Two Dimensional Results

The first objective was to verify the finite element formulation and investigate the fineness of the mesh necessary to obtain accurate results for b and c as functions of frequency. In order to do so, the first case considered was a pore volume consisting of a plane layer of fluid parallel to the direction of the oscillatory motion. For this case, an exact solution for the fluid motion, and thus for b and c, can be obtained (Bedford 1986).

An example of the mesh used for this case is shown in Fig. 3. In Fig. 4, the computed values of the dimensionless displacement $\tilde{u} = u/D$ (crosses) are compared to the exact distribution across the layer for a frequency of 100 Hz. At this relatively low frequency the distribution is essentially a Poiseuille one, and the agreement of the finite element solution with the exact solution is excellent. In Fig. 5, the computed displacement distribution is compared to the exact distribution for a frequency of 100 kHz. In this case, a relatively coarse mesh was used (10 elements across the layer), and the agreement with the exact solution deteriorates near the wall. In Fig. 6, the same case is presented with a mesh of 20 elements across the layer, and the displacement distribution near the wall is modeled accurately.

In Figs. 7 and 8, the values of b and c obtained using the computed displacement distributions for a layer of fluid are compared to the values obtained using the exact distributions. Computations are shown for two values of the layer thickness. These results illustrate the accuracy of the finite element computations. In Figs. 9 and 10, the same results are presented as plots of $b/(\omega\phi\rho_f)$ and $c/(\phi\rho_f)$ as functions of the dimensionless frequency Re. In these two figures the scaling discussed in the previous section is illustrated. The results for three values of the layer thickness fall on a single curve.

An important result that was observed is that *the values of b and c were approximately constant (independent of frequency) up to a value of Re of approximately* 10.

Another case that was considered was chosen to be a two dimensional approximation of the pore space in a porous medium consisting of spherical grains. The geometry was a periodic array of cylinders with porosity $\phi = 0.365$. The periodic "microelement" and the finite element mesh used for this case are shown in Fig. 11. An important question that was investigated

in this two dimensional study was the sensitivity of the computed values of b and c to the shape of the "grains" of the porous medium. For this purpose computations were also carried out for three other geometries, each having the same porosity (0.365).

- A periodic array of square rods. The periodic element and mesh are shown in Fig. 12. The motion was horizontal; thus the rods were "diamond shaped."
- A periodic array of irregularly shaped rods with elongation oriented horizontally. The periodic element and mesh are shown in Fig. 13.
- The periodic array of irregularly shaped elements with elongation oriented vertically.

The results for $b/(\omega\phi\rho_f)$ and $c/(\phi\rho_f)$ as functions of dimensionless frequency Re for the various shapes are shown in Figs. 14 and 15. The characteristic dimension D was chosen to be the minimum gap width between the rods. The value of D used in the case of the array of square rods was 0.0451 mm. The value of D used for the other shapes was 0.0224 mm. From the results it is seen that the drag coefficient is remarkably insensitive to the geometry of the pore space. (It is important to recall that the porosity was the same in each geometry. In each geometry except the square rods, the minimum gap between the rods was the same.) By contrast, the virtual mass coefficient is seen to be very sensitive to the geometry. However, for both coefficients, the qualitative dependence on the frequency of the various geometries is very similar.

Conclusions

It has been found feasible to use the finite element method together with the method of Bedford, Costley & Stern to obtain accurate values of the Biot drag and virtual mass coefficients as functions of frequency. Within a particular range of frequency, the results can be scaled to obtain the coefficients as functions of frequency for other values of a characteristic dimension of the pore geometry. The computed values of the coefficients

are approximately constant (independent of frequency) up to a value of dimensionless frequency Re of approximately 10.

When computations were carried out for various pore geometries holding the porosity fixed, the drag coefficient was found to be very insensitive to changes in geometry while the virtual mass coefficient was found to be quite sensitive to the geometry. However, the qualitative dependence of both coefficients on frequency was quite similar for the various geometries, suggesting that it may be possible to use empirical "shape factors" to account for pore geometry.

The ultimate objective of this research is to determine the Biot drag and virtual mass coefficients as functions of frequency for three dimensional pore spaces. The results reported in this paper suggest that it will be feasible to do so.

Acknowledgements

This work was supported by the Office of Naval Research. The authors wish to thank Mr. Jack Heacock of ONR for his support and suggestions. The project would not have been possible without the generous help of Professor Eric B. Becker of the University of Texas at Austin, who taught us the foundations of the finite element method and permitted us to use his program TEXLESP.

References

BECKER, E. B., CAREY, G. F., & ODEN, J. T. 1981 *Finite Elements Vol. I, An Introduction.* Prentice-Hall, Inc., Englewood Cliffs, New Jersey.

BEDFORD, A. 1986 Application of Biot's equations to a medium of alternating fluid and solid layers. *J. Wave-Material Interaction* **1**, 34–53.

BEDFORD, A., COSTLEY, R. D., & STERN, M. 1984 On the drag and virtual mass coefficients in Biot's equations. *J. Acoust. Soc. Am.* **76**, 1804–1809.

BERRYMAN, J. G. 1969 Confirmation of Biot's theory. *Appl. Phys. Lett.* **37**, 382–384.

BIOT, M. A. 1956a Theory of elastic waves in a fluid saturated porous solid, I. Low frequency range. *J. Acoust. Soc. Am.* **28**, 168–178.

BIOT, M. A. 1956b Theory of elastic waves in a fluid saturated porous solid, II. Higher frequency range. *J. Acoust. Soc. Am.* **28**, 179–191.

HERMANN, L. R. 1965 Elasticity equations for incompressible and nearly incompressible materials by a variational theorem. *J. Am. Inst. Aero. Astro.* **3**, 1896–1900.

HOVEM, J. M.,& INGRAM, J. D. 1979 Viscous attenuation of sound in saturated sand. *J. Acoust. Soc. Am.* **66**, 1807–1812.

JOHNSON, D. L., & PLONA, T. J. 1982 Acoustic slow waves and the consolidation transition. *J. Acoust. Soc. Am.* **72**, 556–565.

STOLL, R. D. 1977 Acoustic waves in ocean sediments. *Geophysics* **42**, 179–191.

STOLL, R. D., & BRYAN, G. M. 1969 Wave attenuation in saturated sediments. *J. Acoust. Soc. Am.* **47**, 1440–1447.

Figure Captions

Fig. 1. Phase velocity of the Biot fast wave and the first mode of the exact solution.

Fig. 2. Attenuation of the Biot fast wave and the first mode of the exact solution.

Fig. 3. A finite element mesh for a plane layer of fluid.

Fig. 4. Computed and exact displacement distribution at 100 Hz.

Fig. 5. Computed and exact displacement distribution at 100 kHz with 10 elements across the layer.

Fig. 6. Computed and exact displacement distribution at 100 kHz with 20 elements across the layer.

Fig. 7. Computed and exact values of b as functions of frequency.

Fig. 8. Computed and exact values of c as functions of frequency.

Fig. 9. Computed and exact values of $b/\omega\phi\rho_f$ as functions of Re.

Fig. 10. Computed and exact values of $c/\phi\rho_f$ as functions of Re.

Fig. 11. Periodic element and mesh for an array of cylinders.

Fig. 12. Periodic element and mesh for an array of square rods.

Fig. 13. Periodic element and mesh for an array of irregularly shaped rods.

Fig. 14. The dimensionless drag coefficient as a function of dimensionless frequency for various pore geometries.

Fig. 15. The dimensionless virtual mass coefficient as a function of dimensionless frequency for various pore geometries.

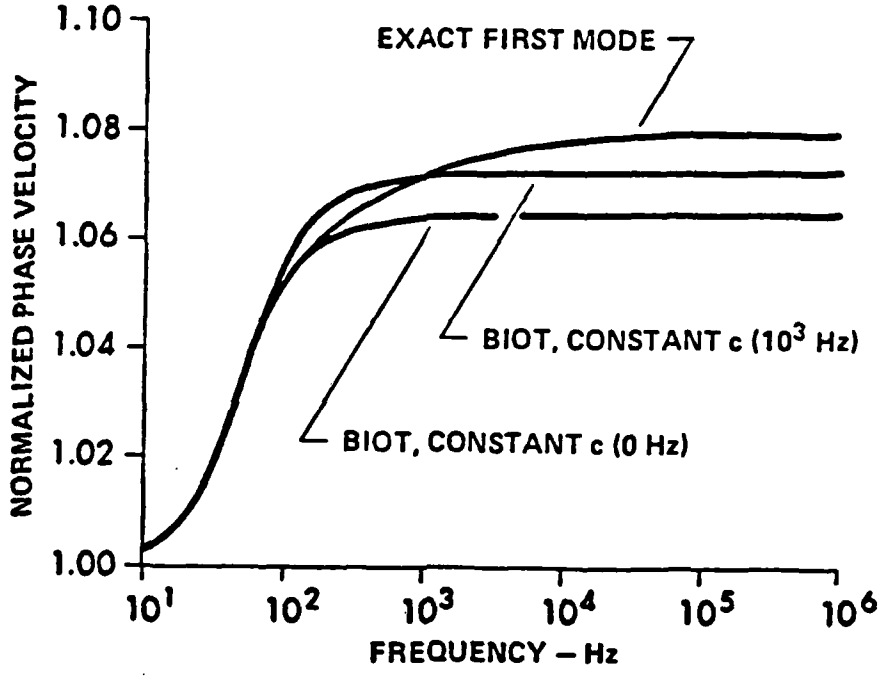

Figure 1: Phase velocity of the Biot fast wave and the first mode of the exact solution

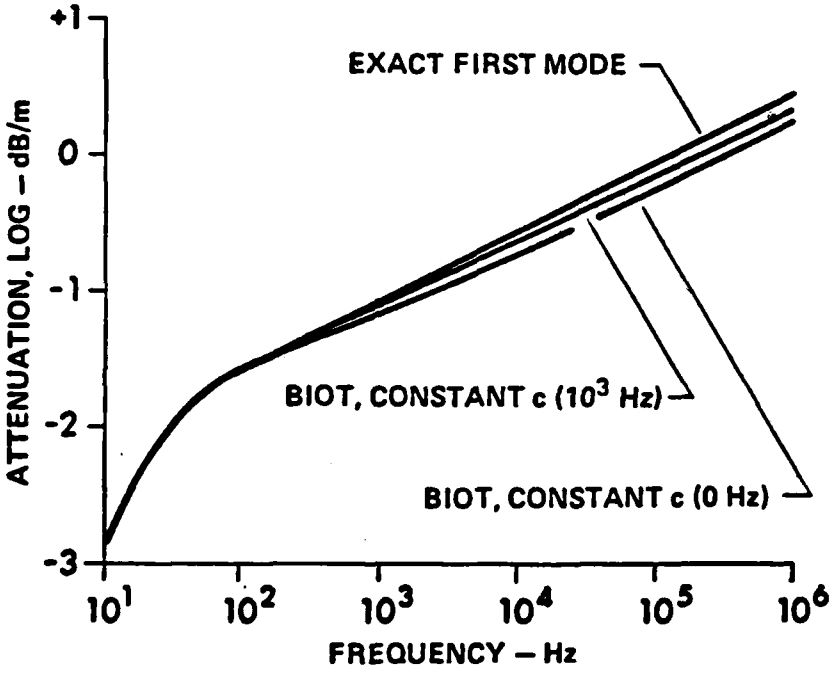

Figure 2: Attenuation of the Biot fast wave and the first mode of the exact solution

Figure 3: A finite element mesh for a plane layer of fluid.

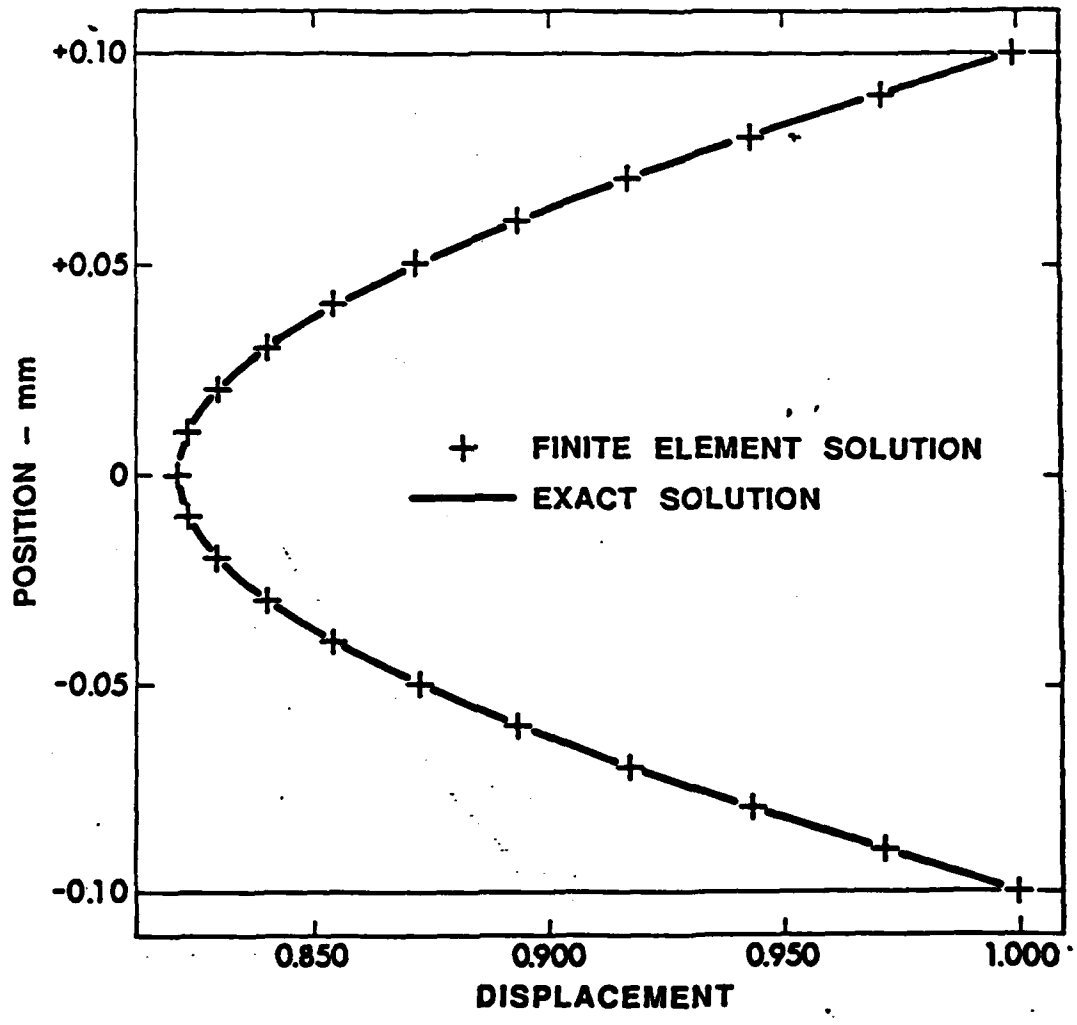

Figure 4: Computed and exact displacement distribution at 100 Hz.

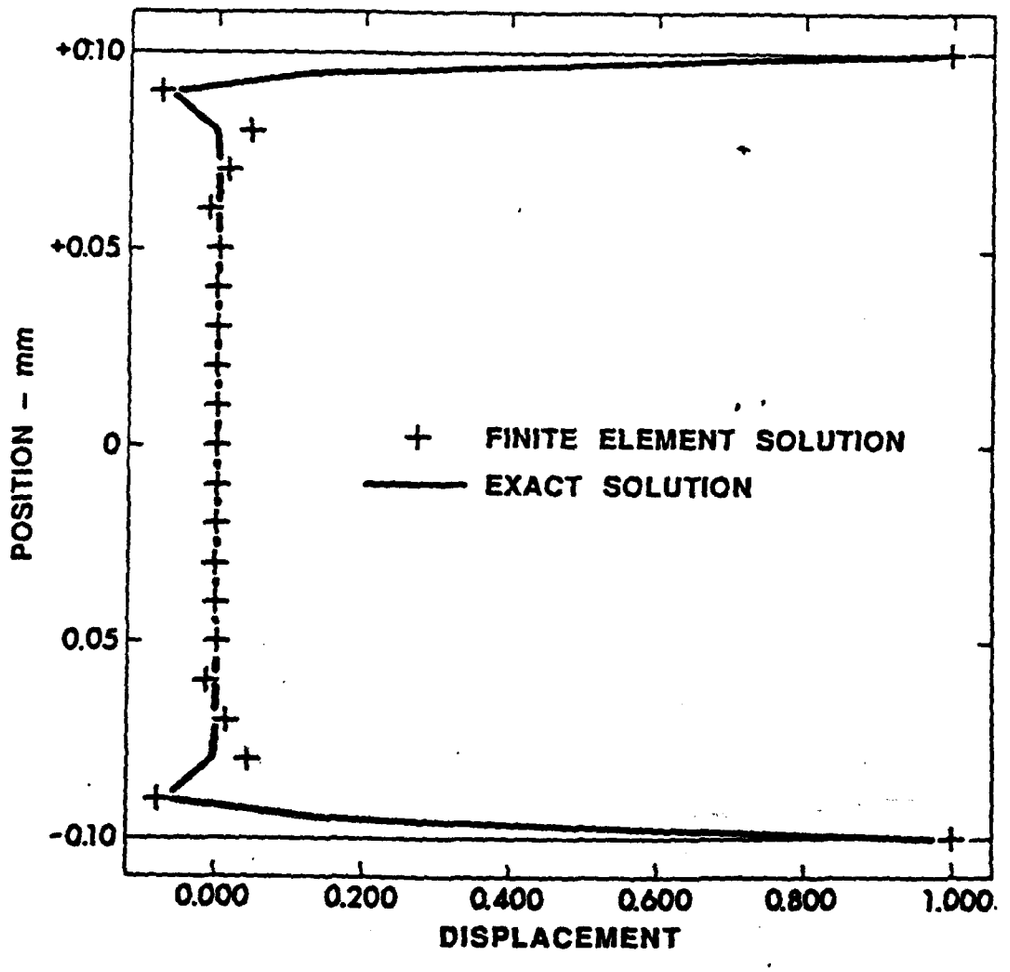

Figure 5: Computed and exact displacement distribution at 100 kHz with 10 elements across the layer.

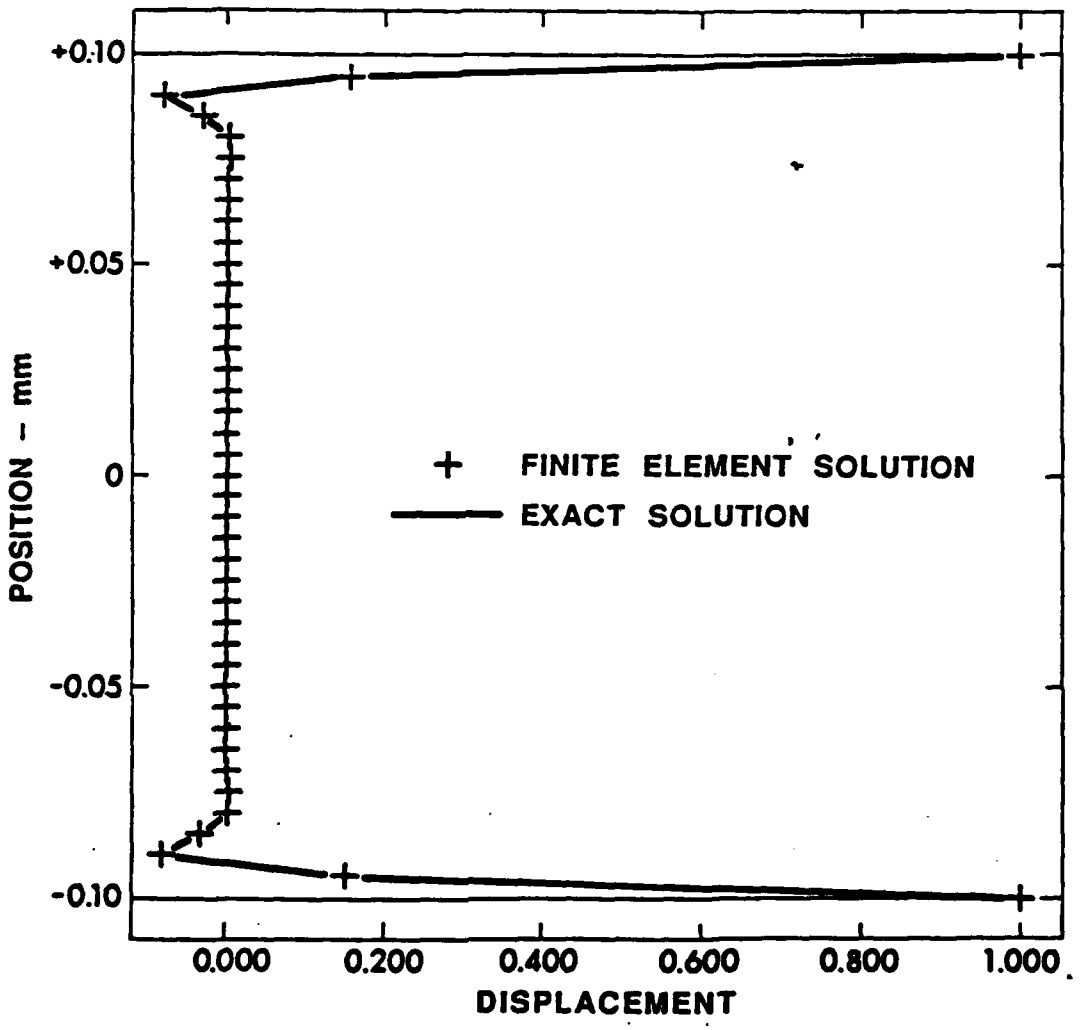

Figure 6: Computed and exact displacement distribution at 100 kHz with 20 elements across the layer.

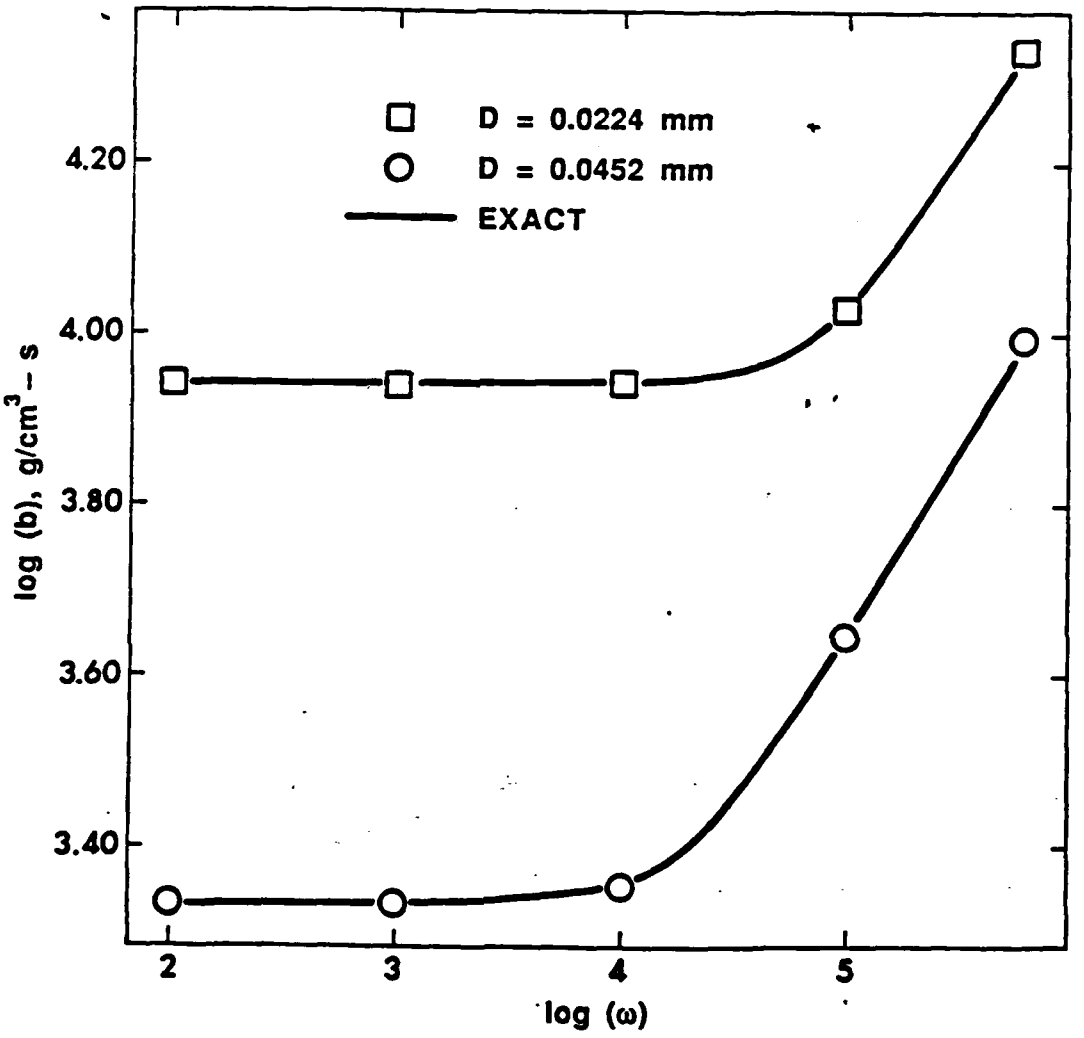

Figure 7: Computed and exact values of b as functions of frequency.

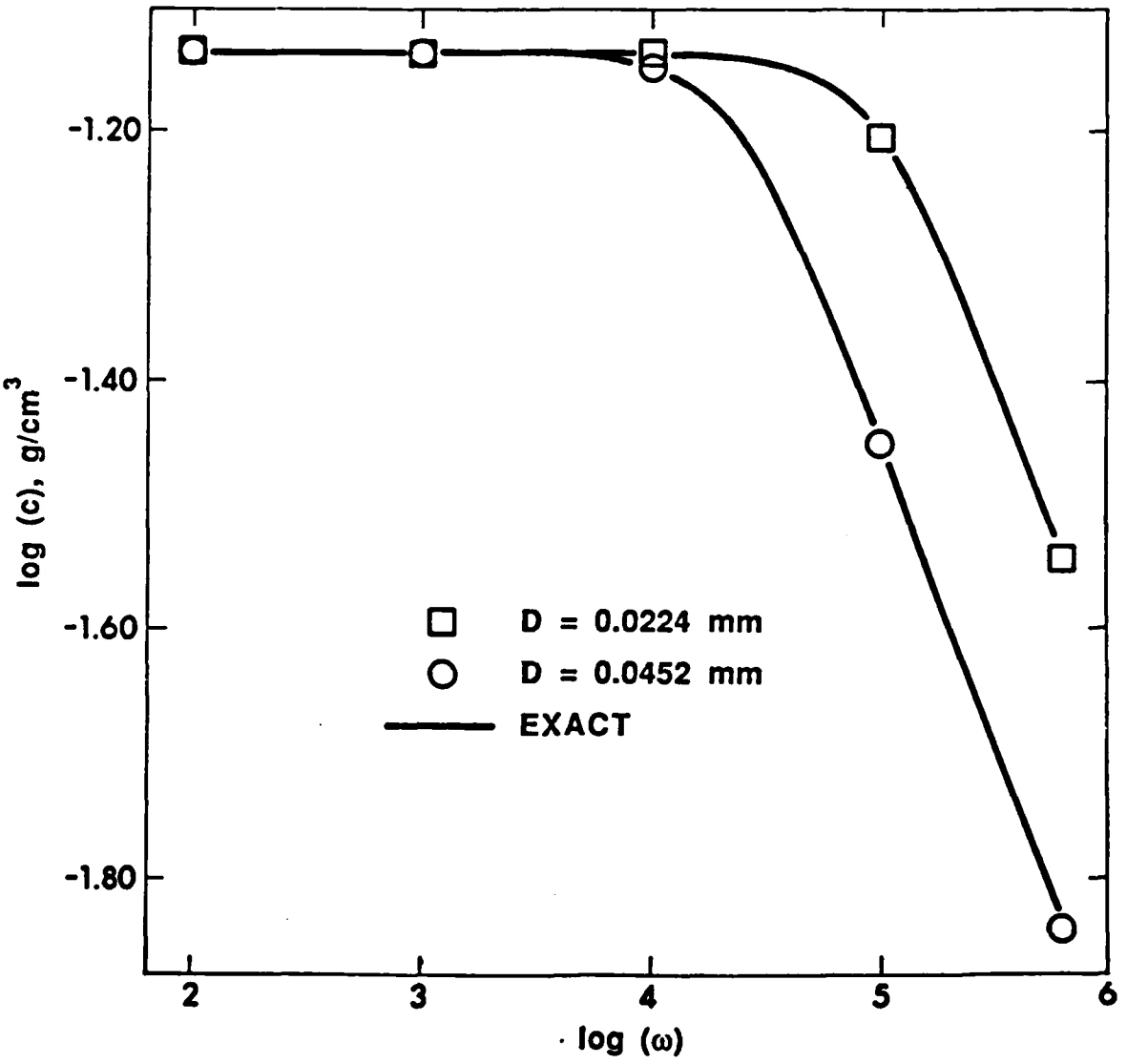

Figure 8: Computed and exact values of c as functions of frequency.

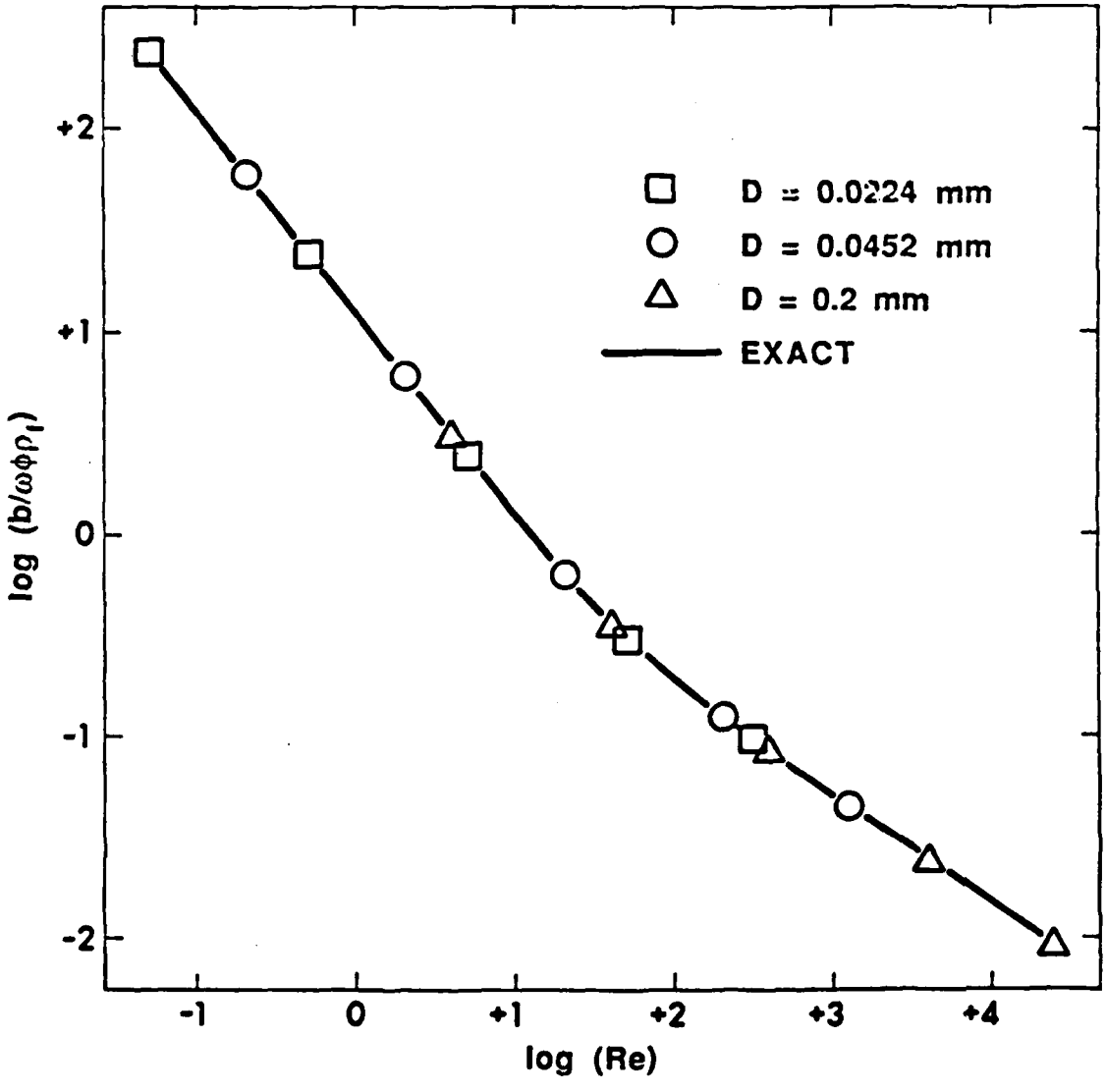

Figure 9: Computed and exact values of $b/\omega\phi\rho_f$ as functions of Re.

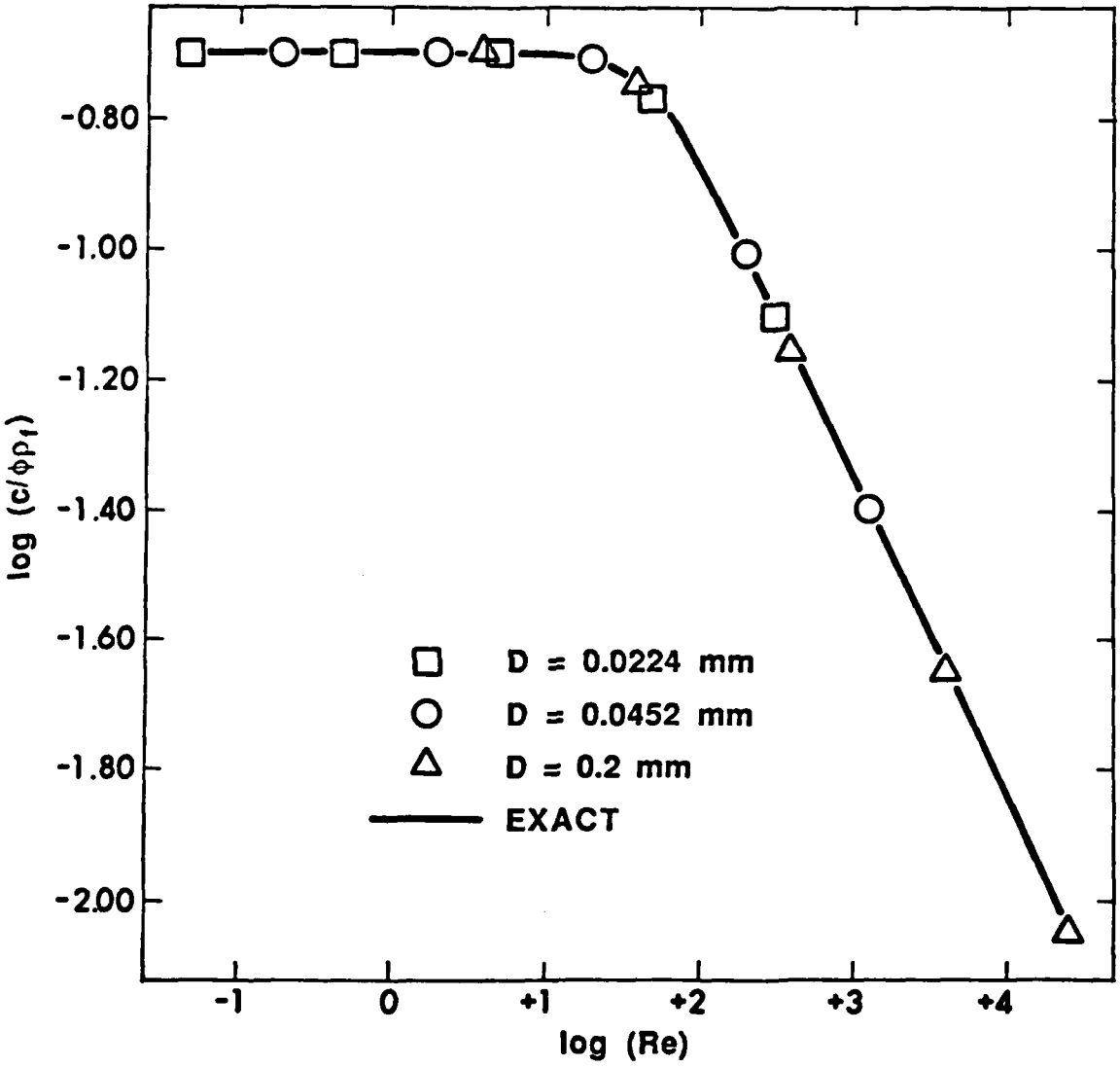

Figure 10: Computed and exact values of $c/\phi\rho_f$ as functions of Re.

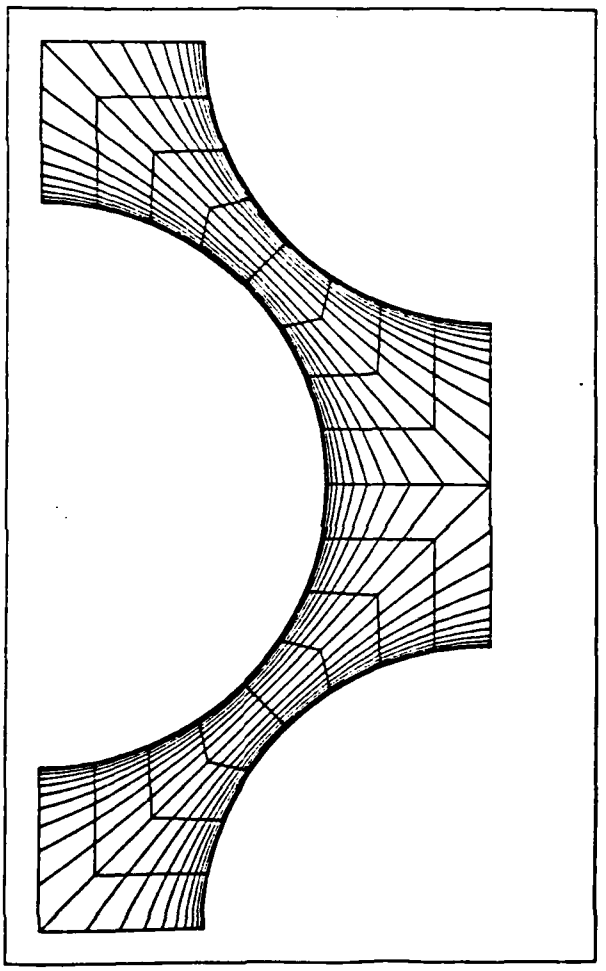

Figure 11: Periodic element and mesh for an array of cylinders.

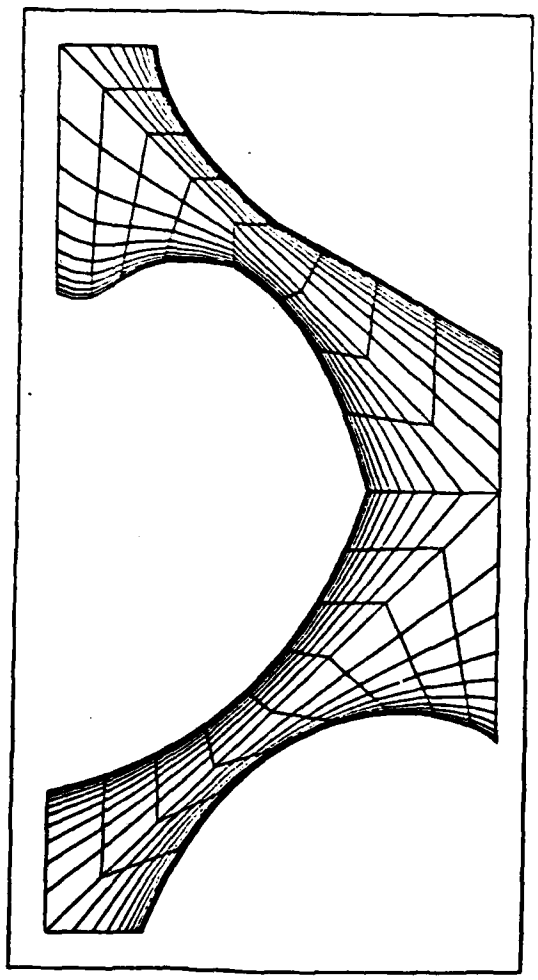

Figure 13: Periodic element and mesh for an array of irregularly shaped rods.

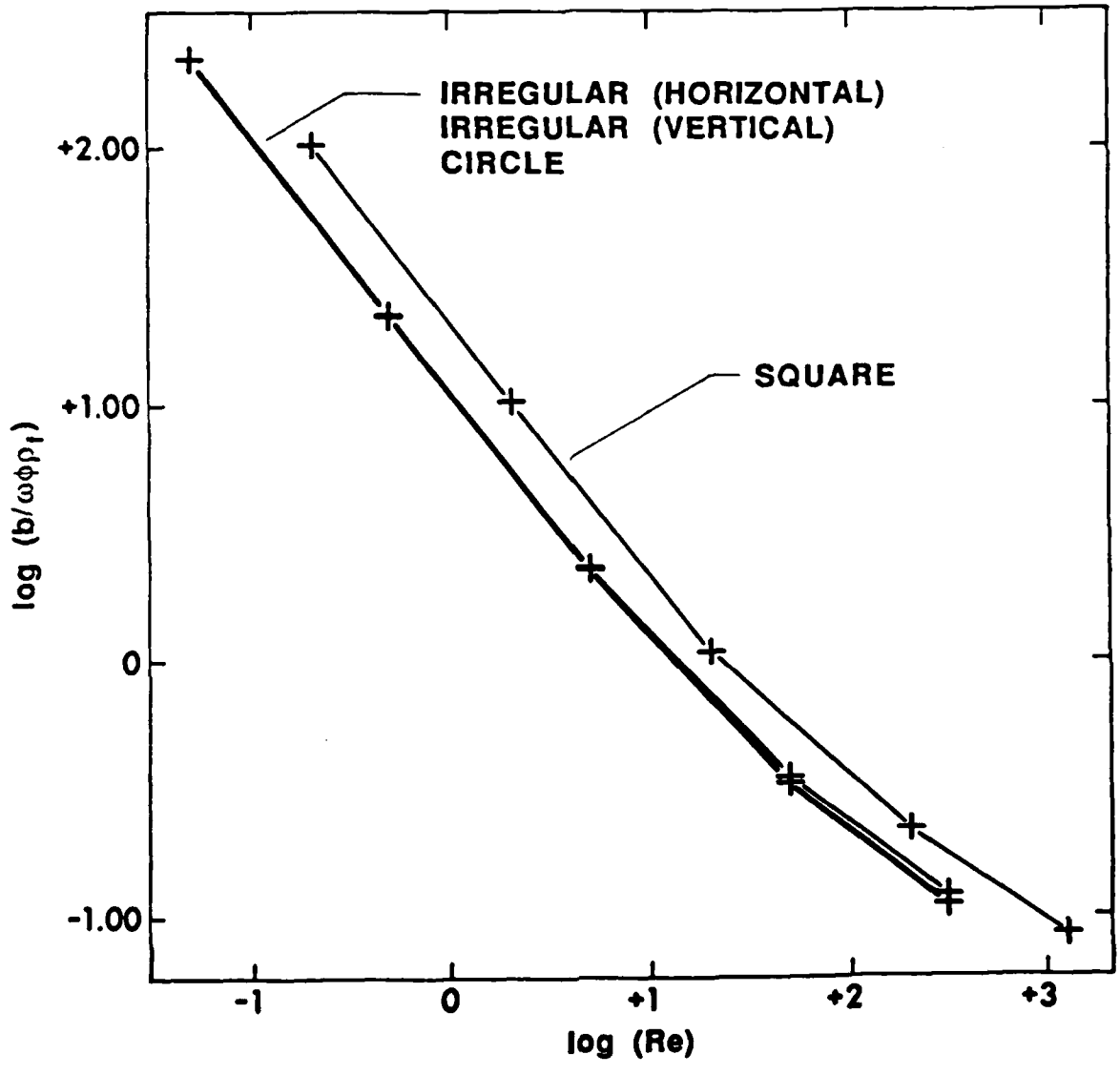

Figure 14: The dimensionless drag coefficient as a function of dimensionless frequency for various pore geometries.

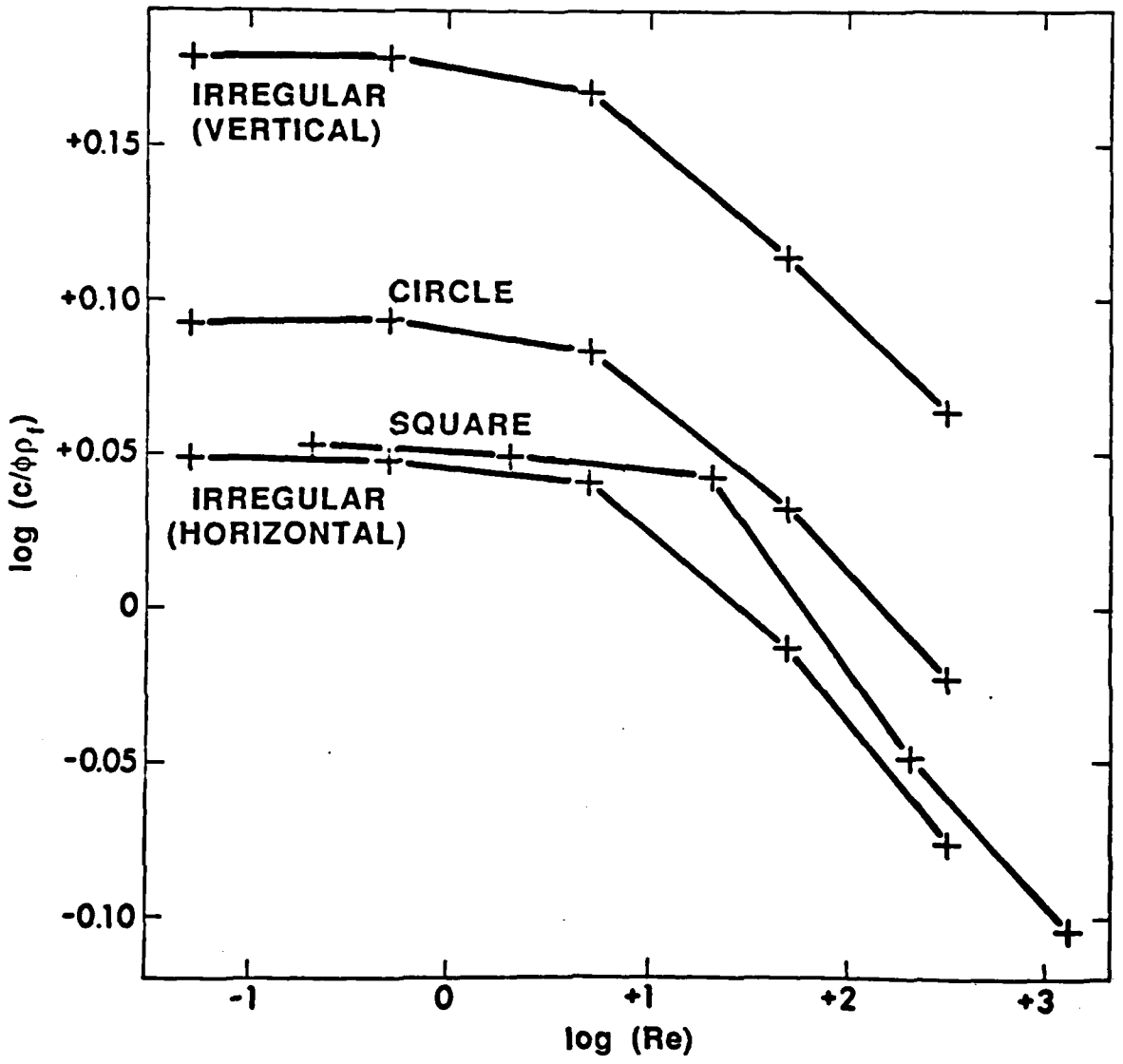

Figure 15: The dimensionless virtual mass coefficient as a function of dimensionless frequency for various pore geometries.

END
DATE
FILMED
5—88
DTIC